Monte Carlo Project - Heston Numerical Schemes

Benjamin Cohen - Nicolas Gros

July 6, 2024

Abstract

This paper implements numerical schemes of both low and high order derived from seminal works in stochastic differential equations (SDEs) approximation: S. Ninomiya and N. Victoir's weak approximation method and A. Alfonsi's high order discretization schemes [NV08, Alf10]. To achieve this, we rely on the following articles: "Weak approximation of stochastic differential equations and application to derivative pricing" [NV08] and "High order discretization schemes for the CIR process: application to affine term structure and Heston models" [Alf10]. The aim is to implement the numerical scheme introduced in these articles for pricing in the Heston model. Comparative analysis includes the Euler scheme alongside various variance reduction techniques. This research aims also to evaluate the efficacy of these schemes in accurately pricing derivatives. Key findings are expected to contribute to enhancing computational efficiency and accuracy in derivative pricing.

1 Introduction

1.1 Focus on Ninomiya and Victoir's article

Ninomiya and Victoir consider a stochastic differential equation written in the Stratonovich form

$$Y(t,x) = x + \int_0^t V_0(Y(s,x))\,ds + \sum_{i=1}^{d} \int_0^t V_i(Y(s,x)) \circ dB_i(s),$$

where $B = (B_1, \ldots, B_d)$ represents a standard Brownian motion, and $V_j \in C_b^\infty(\mathbb{R}^N; \mathbb{R}^N)$, with N denoting the dimensionality. This formulation allows us to study the evolution of stochastic processes and is particularly relevant in derivative pricing within financial models such as the Heston model.

It is also important to emphasize that this is not an Ito integral. However, the process that will interest us later in this paper (expressed as an Ito integral) can be put into the form of a Stratonovich integral.

1.2 Focus on Alfonsi's article

Alfonsi's paper tackles discretization methods for the CIR process and related diffusion models, crucial in finance. It acknowledges the computational challenges of exact simulation methods and highlights the need for efficient discretization, especially when simulating processes over time grids. Alfonsi introduces novel discretization schemes capable of handling large volatility values, providing rigorous theoretical analyses. The paper's structure includes an introduction to notation, assumptions, and weak error analysis, followed by the construction and application of these schemes to various models, showcasing their effectiveness through simulation results. In essence, Alfonsi's work offers practical solutions for accurately simulating financial processes with significant volatility coefficients. We will use in this paper the following parametrization of the CIR process:

$$\begin{aligned} dX_t &= (\alpha - kX_t)dt + \sigma\sqrt{X_t}dW_t, \quad t \in [0,T], \\ X_0 &= x \geq 0, \end{aligned} \tag{1}$$

with parameters $(\alpha, k, \sigma) \in \mathbb{R}_+^* \times \mathbb{R} \times \mathbb{R}_+$. It is a nonnegative process. Moreover, if $x > 0$ and $2\alpha \geq \sigma^2$, the process $(X_t, t \geq 0)$ is always positive. We will exclude the trivial case $\sigma = 0$ and assume $\sigma > 0$ in the whole paper.

The paper addresses challenges in discretizing the CIR process, focusing on issues near zero where traditional methods fail. It reviews recent research on specialized schemes but emphasizes the need for solutions accommodating large volatility coefficients. The paper introduces efficient second and third-order schemes for the CIR process, offering theoretical analysis and practical applicability. It also presents a recursive method for broader diffusion models. Structured sections cover notation, weak error analysis, scheme construction, application to other models, and simulation results, particularly options pricing. Overall, the paper offers promising solutions for handling significant volatility in financial modeling.

2 First Order Discretization Scheme

2.1 Euler-Maruyama scheme

One of the most widely used probabilistic methods for approximating the expected value $E[f(Y(T,x))]$ is the Euler-Maruyama method. This method involves discretizing the stochastic differential equation and iteratively updating the solution using random variables sampled from suitable distributions. Despite its simplicity, the Euler-Maruyama method exhibits convergence properties, albeit with limitations in higher dimensions.

For example, let us first consider the following simple case:

$$dX_t = \alpha dt + \sigma dW_t.$$

Let $t_0 = 0$, $X_0^n = x$, $t_i = i\Delta t$ for $\Delta t > 0$ a fixed time step, and $t_n = T$ the maturity. We define:

$$\begin{aligned} X_{t_0}^n &= x, \\ X_{t_{n+1}}^n &= X_{t_n} + \alpha(t_{n+1} - t_n) + \sigma(W_{t_{n+1}} - W_{t_n}) \\ &= \alpha\Delta t + \sigma\sqrt{\Delta t} Z_{n+1}, \end{aligned}$$

where $(Z_n)_{n\geq 1}$ is a sequence of i.i.d. standard Gaussian random variables.

Then, the expected value $E[f(Y(T,x))]$ is obtained by Monte Carlo or Quasi-Monte Carlo (by computing many paths of the process X).

2.2 Application to the pricing of an Asian Call in Heston model

In Ninomiya and Victoir's article, this method is applied to the pricing of an Asian call with maturity T and strike K in the Heston model, i.e. such that:

$$Y_1(t,x) = x_1 + \int_0^t \mu Y_1(s,x)ds + \int_0^t Y_1(s,x)\sqrt{Y_2(s,x)}dB_1(s)$$

$$Y_2(t,x) = x_2 + \int_0^t \alpha(\theta - Y_2(s,x))ds + \int_0^t \beta\sqrt{Y_2(s,x)}dB_2(s)$$

$$Y_3(t,x) = \int_0^t Y_1(s,x)ds$$

where $x = (x_1, x_2) \in \mathbb{R}^{>0}$, $(B_1(t), B_2(t))$ is a 2-dimensional standard Brownian motion, and α, θ, μ are some positive coefficients such that $2\alpha\theta - \beta^2 > 0$ to ensure the existence and uniqueness of a solution to our SDE.

The aim is to compute $\mathbb{E}(\frac{1}{T}Y_3(T,x) - K)_+$. The Euler-Maruyama scheme is:

$$Y_1(t_{i+1},x) = Y_1(t_i,x) + Y_1(t_i,x)\mu(t_{i+1} - t_i) + Y_1(t_i,x)\sqrt{Y_2(t_i,x)}(dB_1(t_{i+1}) - dB_1(t_i))$$

$$Y_2(t_{i+1},x) = Y_2(t_i,x) + \alpha(\theta - Y_2(t_i,x))(t_{i+1} - t_i) + \beta\sqrt{Y_2(t_{i+1},x)}(dB_2(t_{i+1}) - dB_2(t_i))$$

$$Y_3(t_{i+1},x) = Y_3(t_{i+1},x) + Y_1(t_i,x)(t_{i+1} - t_i)$$

Finally, se can the easily compute many paths of Y_3 and compute the empirical mean of $(\frac{1}{T}Y_3(T,x) - K)_+$ for all paths.

2.3 A remark on the Monte Carlo method

The Monte Carlo method provides a powerful tool for numerical approximation, particularly in high-dimensional spaces. Moreover, if one uses Monte Carlo, one also can compute the empirical variance to get a confidence interval.

2.4 A remark on the quasi-Monte Carlo method

The quasi-Monte Carlo method offers an alternative to traditional Monte Carlo approaches, potentially reducing the computational burden in certain scenarios. However, its effectiveness depends heavily on the dimensionality of the integration space and the specific problem at hand.

To implement a quasi-Monte Carlo method, we need to choose a sequence with low dicrepancy (such as the Sobol or Halton sequence). These sequences are uniformly distributed over the interval $[0, 1]$. If we want to generate Gaussian variables, we simply invert the distribution function of the Gaussian distribution to obtain our variables.

Moreover, since the low-discrepancy sequence we are using is deterministic, it is very important to generate all the necessary variables at the start of the run to ensure that we do not select the same terms twice.

To carry out our simulations, we used the Sobol suite.

3 Romberg Extrapolation

Romberg extrapolation offers a systematic approach to improve the accuracy of approximation schemes. By recursively applying corrections to lower-order approximations, Romberg extrapolation enhances convergence rates, leading to more accurate estimations of the expected value.

Consider a nice scheme of order p, that is, a scheme $X_{k/n}^{(\text{ord } p),n}$ such that for smooth f, there exists a constant K_f such that

$$\left| E\left[f\left(X_1^{(\text{ord } p),n} \right) \right] - E\left[f(Y(1,x)) \right] - \frac{K_f}{n^p} \right| \leq C_f \frac{1}{n^{p+1}}. \tag{2}$$

Then,

$$\frac{2^p}{2^p - 1} E\left[f\left(X_1^{(\text{ord } p),2n} \right) \right] - \frac{1}{2^p - 1} E\left[f\left(X_1^{(\text{ord } p),n} \right) \right] \tag{3}$$

provides a scheme of order $p + 1$.

The key idea behind Romberg extrapolation is to combine the results of multiple discretization steps with different time step sizes to obtain a more accurate estimate. The method works as follows:

- Discretize the stochastic process using with a given discretization scheme with an initial number of time steps, n. This gives a first approximation of the process.
- Repeat the this discretization scheme with a larger number of time steps, multiplied by 2 ($2n$, $4n$, etc). We save the results in a Romberg table and we apply the Romberg extrapolation formula given by $R_{i,j} = R_{i,j-1} + \frac{R_{i,j-1} - R_{i-1,j-1}}{4^{j-1}-1}$, where $R_{i,j}$ is the Romberg extrapolated value at level j and column i.
- The final value is given by $R_{n,n}$

In our project, the Romber extrapolation will be applied to Euler-Maruyama scheme but also to he Ninomiya and Victoir's scheme.

4 Second Order Discretization Scheme for SDEs in Stratonovich form

4.1 The SDE in Stratonovich form

We consider a stochastic differential equation written in the Stratonovich form

$$Y(t,x) = x + \int_0^t V_0(Y(s,x))\,ds + \sum_{i=1}^{d} \int_0^t V_i(Y(s,x)) \circ dB_i(s),$$

where $B = (B_1, \ldots, B_d)$ represents a standard Brownian motion.

4.2 The discretization scheme of Ninomiya and Victoir

Let $(\Lambda_i, Z_i)i \in 1, \ldots, n$ be n independent random variables, where each Λ_i is a Bernoulli random variable independent of Z_i, which is a standard d-dimensional normal random variable. Define $(X^{\mathrm{New},n}_{\frac{k}{n}})_{k=0,\ldots,n}$ to be a family of random variables as follows:

$$X^{\mathrm{New},n}_{\frac{k+1}{n}} = \begin{cases} \exp\left(\frac{V_0}{2n}\right) \exp\left(\sum_{i=1}^{d} \frac{Z_k^i V_i}{\sqrt{n}}\right) X^{\mathrm{New},n}_{\frac{k}{n}} & \text{if } \Lambda_k = +1 \\ \exp\left(\frac{V_0}{2n}\right) \exp\left(\sum_{i=1}^{d} \frac{Z_k^i V_i}{\sqrt{n}}\right) X^{\mathrm{New},n}_{\frac{k}{n}} & \text{if } \Lambda_k = -1 \end{cases} \tag{4}$$

The notation $\exp(V)x$ denotes the solution at time 1 of the ordinary differential equation:

$$\frac{dz_t}{dt} = V(z_t), \quad z_0 = x, \tag{5}$$

for V a smooth vector field.

4.3 An important result about this algorithm

For all $f \in C_b^\infty(\mathbb{R}^N)$, we have:

$$\left| E\left[f\left(X_1^{(\mathrm{New}),n} \right) \right] - E\left[f(Y(1,x)) \right] \right| \leq \frac{C_f}{n^2} \tag{6}$$

As a consequence, this discretization scheme is of order 2.

4.4 Application to the pricing of an Asian Call in Heston model

We consider again the following stochastic differential equations:

$$Y_1(t,x) = x_1 + \int_0^t \mu Y_1(s,x) ds + \int_0^t Y_1(s,x)\sqrt{Y_2(s,x)} dB_1(s)$$

$$Y_2(t,x) = x_2 + \int_0^t \alpha(\theta - Y_2(s,x)) ds + \int_0^t \beta\sqrt{Y_2(s,x)} dB_2(s)$$

$$Y_3(t,x) = \int_0^t Y_1(s,x) ds$$

where $x = (x_1, x_2) \in \mathbb{R}^{>0}$, $(B_1(t), B_2(t))$ is a 2-dimensional standard Brownian motion, and α, θ, μ are some positive coefficients such that $2\alpha\theta - \beta^2 > 0$ to ensure the existence and uniqueness of a solution to our SDE.

Then, we can transform these SDEs into Stratonovich form:

$$Y(t,x) = \sum_{i=0}^{2} \int_0^t V_i(Y(s,x)) \circ dB_i(s), \tag{7}$$

where

$$V_0(t, y_1, y_2, y_3) = {}^t\left(y_1\mu - \frac{y_2^2}{2} \right),$$

$$V_1(t, y_1, y_2, y_3) = {}^t\left(y_1\sqrt{y_2}, 0, 0 \right),$$

$$V_2(t, y_1, y_2, y_3) = {}^t\left(0, \beta\sqrt{y_2}, 0 \right).$$

Solutions of the ODEs We can get $\exp(sV_1)$ and $\exp(sV_2)$ as follows:

$$\exp(sV_1)\ {}^t(y_1,y_2,y_3) = {}^t\left(e^{s\sqrt{y_2}}, y_2, y_3\right),$$
$$\exp(sV_2)\ {}^t(y_1,y_2,y_3) = {}^t\left(y_1, y_2, \beta s^2 + \sqrt{y_2}^2\right).$$

However, there exists no closed-formula for $\exp(sV_0)$. We are forced to use an approximation and Ninomiya and Victoir choose:

$$\exp(sV_0)\ {}^t(y_1,y_2,y_3) = {}^t(g_1(s), g_2(s), g_3(s)),$$

where

$$g_1(s) = y_1 \exp\left(\mu - \frac{J^2}{2}\right) s + y_2 - \frac{J^2}{2\alpha}\left(e^{-\alpha s} - 1\right),$$
$$g_2(s) = J + (y_2 - J)\, e^{-\alpha s},$$
$$g_3(s) = y_3 + y_1\left(e^{As} - 1\right) A + O(s^3),$$
$$J = \theta - \frac{\beta^2}{4\alpha}, \quad A = \mu - \frac{y_2^2}{2}.$$

In the general case In general, it is not always possible to obtain the closed-formula of $\exp(sV_i)$. Even in such cases, we have to find an approximation of $\exp(sV_0)$ whose error is $O(s^3)$ and approximations of $\exp(sV_i)$ whose errors are $O(s^6)$. This is essential for our algorithm to be of order 2. This can be achieved by Runge-Kutta-like methods for example.

4.5 A remark on the Monte Carlo method

In this algorithm, we need independent standard normal random variables and independent Bernoulli random variables. To compute the price of our Asian call with payoff $(\frac{1}{T}Y_3(T,x) - K)_+$, we just have to generate many results for $Y_3(T,x)$ and then take the empirical mean of the payoff. One also can compute the empirical variance to get a confidence interval.

4.6 A remark on the quasi-Monte Carlo method

The quasi-Monte Carlo method ca be done on this algorithm. We have to generate $(\Lambda_i, Z_i)_{i\in\{1,\dots,n\}}$ into $[0,1)^{n(d+1)}$.

Here again, since the low-discrepancy sequence we are using is deterministic, it is very important to generate all the necessary variables (Bernoulli variables and normal variables) at the start of the run to ensure that we do not select the same terms twice.

To carry out our simulations, we used the Sobol suite.

5 Second Order Discretization Schemes for SDEs in Ito form

5.1 Assumptions on the SDE and Notation

d_W-dimensional standard Brownian motion $(W_t, t \geq 0)$. $(F_t)_{t\geq 0}$ its augmented associated filtration.
$d \in \mathbb{N}^*$, $D \subset \mathbb{R}^d$ a product of d intervals. For example $D = \mathbb{R}_+^{d_1} \times \mathbb{R}^{d_2}$ with $d_1 + d_2 = d$.
$\forall \alpha = (\alpha_1, ..., \alpha_d) \in \mathbb{N}^d$, $\partial^\alpha = \partial_1^{\alpha_1} \cdots \partial_d^{\alpha_d}$ and $|\alpha| = \sum_{l=1}^d \alpha_l$.

$$C^\infty_{\text{pol}}(D) = \{f \in C^\infty(D,\mathbb{R}) \mid \forall \alpha \in \mathbb{N}^d, \exists C_\alpha > 0, e_\alpha \in \mathbb{N}^*, \forall x \in D, \quad |\partial^\alpha f(x)| \leq C_\alpha(1 + \|x\|^{e_\alpha})\},$$

$(C_\alpha, e_\alpha)_{\alpha\in\mathbb{N}^d}$ is a good sequence for $f \in C^\infty_{\text{pol}}(D)$ if $\forall x \in D, |\partial^\alpha f(x)| \leq C_\alpha(1 + \|x\|^{e_\alpha})$.
Assumptions: $b : D \to \mathbb{R}^d$ and $\sigma : D \to \mathbb{M}^{d\times d}(\mathbb{R})$ are such that for $1 \leq i, j \leq d$, the functions $x \in D \to b_i(x)$ and $x \in D \to (\sigma\sigma^*)_{i,j}(x)$ are in $C^\infty_{\text{pol}}(D)$. For $x \in D$, we introduce the general $\mathbb{R}^d$-valued SDE:

$$X_t^x = x + \int_0^t b(X_s^x)ds + \int_0^t \sigma(X_s^x)dW_s. \tag{8}$$

$\forall x \in D, \exists!$ weak solution for $t \geq 0$, and $\mathbb{P}(\forall t \geq 0, X_t^x \in D) = 1$ satisfying the strong Markov property. Differential operator associated to the SDE is given by

$$Lf(x) = \sum_{i=1}^{d} b_i(x)\partial_i f(x) + \frac{1}{2}\sum_{i=1}^{d}\sum_{j=1}^{d}\sum_{k=1}^{dW} \sigma_{i,k}(x)\sigma_{j,k}(x)\partial_i\partial_j f(x). \tag{9}$$

$f \in C_{\text{pol}}^{\infty}(D)$ and conditions on $(b, \sigma) \implies$ iterated $L^k f(x) \in C_{\text{pol}}^{\infty}(D)\ \forall k \in \mathbb{N}$ well defined on D.

Time horizon $T > 0$. Time discretization $t_{ni} = iT/n$ for $i = 0, 1, ..., n$.

Definition: Transition probabilities $(\hat{p}_x(t)(dz), t > 0, x \in D)$ on D are such that $\hat{p}_x(t)$ is a probability law on D for $t > 0$ and $x \in D$.

A discretization scheme with transition probabilities $(\hat{p}_x(t)(dz), t > 0, x \in D)$ is a sequence $(X_{t_{ni}}^{\hat{n}}, 0 \leq i \leq n)$ of D-valued random variables such that:

- $\forall\ 0 \leq i \leq n$, $X_{t_{ni}}^{\hat{n}}$ is an $\mathcal{F}_{t_{ni}}$-measurable random variable on D,
- Law of $X_{t_{ni+1}}^{\hat{n}}$ given by $\mathbb{E}[f(\hat{X}_{t_{i+1}^n}^n) \mid \mathcal{F}_{t_i^n}] = \int f(z)\hat{p}_{X_{t_i^n}^{\hat{n}}}(T/n)(dz)$ depends on $X_{t_i^n}^{\hat{n}}$ and T/n.

$\forall\ t > 0, x \in D$, $\hat{X}_t^x$ follows $\hat{p}_x(t)(dz)$. Discretization scheme $(\hat{X}_{t_i^n}^n, 0 \leq i \leq n)$ determined by initial value and transition probabilities.

Definition: $C_K^{\infty}(D, \mathbb{R})$ set of the C^{∞} real-valued functions with a compact support in D. For $x \in D$. Discretization scheme $(\hat{X}_{t_i^n}^n, 0 \leq i \leq n)$ is a weak νth-order scheme for the SDE $(X_x^t, t \geq 0)$ if:

$$\forall f \in C_K^{\infty}(D, \mathbb{R}), \exists K > 0, \quad |\mathbb{E}(f(X_x^T)) - \mathbb{E}(f(X_{t_{nn}}^{\hat{n}}))| \leq \frac{K}{n^{\nu}}.$$

$\mathbb{E}(f(X_x^T)) - \mathbb{E}(f(X_{t_n^n}^{\hat{n}}))$ is called the weak error associated to f.

5.2 Analysis of the Weak Error

$(\hat{X}_{t_{ni}}^n, 0 \leq i \leq n)$ has uniformly bounded moments if $\exists\ n_0 \forall n_0 \leq n; q \in \mathbb{N}^* : \sup\ \mathbb{E}(\|\hat{X}_{t_i^n}^n\|^q) < \infty$.

If $\exists\ 0 \leq \eta$ such that $\forall t \in (0, \eta)$ and $\forall q \in \mathbb{Z}^+$, $\exists C_q$ such that $\mathbb{E}[(\hat{X}_t^x)^q]$ is bounded by a function involving x^q, multiplied by a term dependent on q and t, then the discretization scheme has uniformly bounded moments.

Previous definition introduces the concept of a remainder of order ν for a given mapping f from $C_{\text{pol}}^{\infty}(D)$ to $\mathbb{R}$. It describes a function Rf such that for any function f with a good sequence $(C_\alpha, e_\alpha)_{\alpha \in \mathbb{N}^d}$, there exist positive constants C, E, and η depending only on the good sequence, satisfying a certain inequality for all t in the interval $(0, \eta)$ and for all x in D.

The theorem presents a key result concerning operators and discretization schemes, stating conditions under which a discretization scheme converges to the expected value of a function in terms of its order and the properties of the scheme and the function.

Then the paper offers extensions of potential weak-order schemes, operators acting on functions, and the behavior of exact schemes.

$\hat{X}_t^x$ νth order weak scheme for L on D, $\implies$ $(\hat{X}_t^x, t)$ potential νth order weak scheme for $L + \partial_t$.

$h \in C_{\text{pol}}^{\infty}(D)$; $f \in C_{\text{pol}}^{\infty}(D \times \mathbb{R})$; $Lhf(x) = L\widetilde{f}(x)$, where $\widetilde{f}(x) = f(x, h(x))$. $\hat{X}_t^x$ νth order weak scheme for L, $\implies$ $(\hat{X}_t^x, h(\hat{X}_t^x))$ potential νth order weak scheme for Lh.

$b : D \to \mathbb{R}^d$ and $\sigma : D \to \mathbb{M}^{d \times dW}(\mathbb{R})$ satisfy $\|b(x)\| + \|\sigma(x)\| \leq C(1 + \|x\|)$ for some $C > 0$, and the associated operator L fulfills the required conditions on D, then the exact scheme serves as a potential weak scheme of order ν for L for any $\nu \in \mathbb{N}$.

The composition of two transition probabilities $\hat{p}_1^x(t)(dz)$ and $\hat{p}_2^x(t)(dz)$ on D is defined as $\hat{p}_2(t_2) \circ \hat{p}_1^x(t_1)(dz) = \int_D \hat{p}_1^y(t_2)(dz)\hat{p}_1^x(t_1)(dy)$ and satisfies certain criteria if the individual probabilities do.

If $\hat{p}_1^x(t)(dz)$ and $\hat{p}_2^x(t)(dz)$ are potential weak νth-order schemes for operators L_1 and L_2, then their composition satisfies certain properties.

5.3 Ninomiya-Victoir Discretization Scheme

If $L_1, \ldots, L_m$ are operators satisfying certain assumptions on D, and $\hat{p}_1^x, \ldots, \hat{p}_m^x$ are potential second-order discretization schemes for these operators, then certain compositions of transition probabilities are potential second-order schemes for the operator $\Sigma L = L_1 + L_2 + \ldots + L_m$.

Under certain conditions on L and $\sigma(x)$, the operator L can be split as $L = V_0 + \frac{1}{2}\sum_{k=1}^{d_W} V_k^2$. This splitting facilitates the resolution of the problem using ordinary differential equations instead of stochastic differential equations.

Under certain conditions, a potential second-order scheme for L can be obtained through a specific composition of transition probabilities and the composition of discretization schemes yields certain properties for the sum of corresponding operators.

5.4 Second Order Scheme for the CIR Process

We focus on discretizing the CIR process with parameters (a, k, σ) and construct a second-order scheme without restrictions on the parameters.

Ninomiya-Victoir's Scheme for the CIR: The operator $LCIR$ is split into V_{CIR}^0 and $\frac{1}{2}(V_{CIR}^1)^2$, allowing for explicit solutions of associated ODEs. When $\sigma^2 \leq 4a$, the Ninomiya-Victoir scheme provides a well-defined second-order scheme. However, for $\sigma^2 > 4a$, the scheme near 0 becomes problematic. By considering different schemes for regions near and away from 0, we ensure non-negativity and define a potential second-order scheme. Propositions are provided to support these claims.

Further analysis involves defining suitable bounded variables and establishing conditions under which the composition scheme remains well-defined and positive, ensuring a potential second-order scheme for the CIR process.

$$X_{CIR}^0(t,x) = xe^{-kt} + \left(a - \frac{\sigma^2}{4}\right)\psi_k(t).$$

$$X_{CIR}^1(t,x) = (\left(\sqrt{x} + \sigma\frac{t}{2}\right)^+)^2, \quad \text{where } (\cdot)^+ \text{ denotes taking the positive part.}$$

$$\psi_k(k,t) = \begin{cases} t & \text{if } k = 0 \\ \frac{1-\exp(-kt)}{k} & \text{otherwise} \end{cases}$$

$$\phi(x,t,w,a,k,\sigma) = \exp\left(-\frac{kt}{2}\right)\left(\sqrt{\left(a - \frac{\sigma^2}{4}\right)\psi_k(k,\frac{t}{2}) + \exp\left(-\frac{kt}{2}\right)x} + \frac{w\sigma}{2}\right)^2 + \left(a - \frac{\sigma^2}{4}\right)\psi_k\left(k,\frac{t}{2}\right)$$

$$K_2(x,t,\sigma,a,k) = \begin{cases} \psi_k(k,\frac{t}{2})\left(\frac{\sigma^2}{4} - a\right) + \left(\sqrt{\exp\left(\frac{kt}{2}\right)\left(\left(\frac{\sigma^2}{4} - a\right)\psi_k(k,\frac{t}{2})\right)} + \frac{\sqrt{3t}\sigma}{2}\right)^2 \text{ if } \sigma^2 > 4a \\ 0 \text{ otherwise} \end{cases}$$

These equations represent the essential components of the Ninomiya-Victoir discretization scheme for the Cox-Ingersoll-Ross (CIR) process, including the functions $\psi_k(t)$ defining time-dependent coefficients, the CIR process components $X_{CIR}^0(t,x)$ and $X_{CIR}^1(t,x)$, and the scheme expression $\phi(x,t,w)$ defining the discretized CIR process. Additionally, $K_2(t)$ serves as a threshold function for the scheme's applicability, ensuring its validity under certain conditions.

5.5 A Potential Second Order Scheme for the CIR process Near 0

To simulate the CIR near 0, we must address challenges arising when $\sigma^2 > 4a$. Preserving nonnegativity is crucial for two reasons: the CIR diffusion is nonnegative, and it ensures well-defined schemes. Extending the process to negative values is complex, and maintaining weak error control is unclear.

Remark 2.6. Extending the CIR process to negative values complicates discretization and weak error control.

To address this, we consider a discrete random variable matching the first two moments. The resulting scheme ensures nonnegativity and is well-defined near 0.

Equations:

$$\tilde{u}_1(t,x) = xe^{-kt} + a\psi_k(t), \tag{10}$$

$$\tilde{u}_2(t,x) = \tilde{u}_1(t,x)^2 + \sigma^2\psi_k(t)\left[\frac{a\psi_k(t)}{2} + xe^{-kt}\right], \tag{11}$$

$$\pi(t,x) = 1 - \frac{\Delta(t,x)}{2}, \tag{12}$$

$$\Delta(t,x) = 1 - \frac{\tilde{u}_1(t,x)^2}{\tilde{u}_2(t,x)}, \tag{13}$$

$$\hat{p}_x(t)(dz) = \left\{\pi(t,x)\delta_{\frac{\tilde{u}_1(t,x)}{2\pi(t,x)}}(dz) + (1-\pi(t,x))\delta_{\frac{\tilde{u}_1(t,x)}{2(1-\pi(t,x))}}(dz) \quad \text{for } 0 \le x < K_2(t) \right. \tag{14}$$

5.6 The Second Order Scheme for the CIR process

Let Y be a random variable such that $P(Y=\sqrt{3}) = P(Y=-\sqrt{3}) = \frac{1}{6}$ and $P(Y=0) = \frac{2}{3}$. $K_2(t)$ and $\phi, \tilde{u}_1(t,x), \pi(t,x)$ defined as above. Then Y matches the first 5 moments of a standard Gaussian.

Let us define for $t>0$, $p^{\hat{x}}(t)(dz)$ the law of $\phi(x,t,\sqrt{t}Y)$ for $x \ge K_2(t)$ and

$$\hat{p}_x(t)(t)(dz) = \left\{\pi(t,x)\delta_{\frac{\tilde{u}_1(t,x)}{2\pi(t,x)}}(dz) + (1-\pi(t,x))\delta_{\frac{\tilde{u}_1(t,x)}{2(1-\pi(t,x))}}(dz) \quad \text{for } 0 \le x < K_2(t) \right.$$

The scheme $(\hat{X}^x_{t^i_n}, 0 \le i \le n)$ associated to the transition probabilities $(\hat{p}_x(t)(dz), t>0)$ and starting from $\hat{X}^x_{t^0_n} = x \in \mathbb{R}^+$ is well defined and nonnegative. A technical result ensures the C^∞ property of the scheme. The theorem follows from the well-defined nature and bounded moments of the scheme. The addition to the scheme proposed by Ninomiya and Victoir is that we have a well-defined second order scheme, without restriction on the parameters.

5.7 The Third Order Scheme for the CIR process

$XCIR\_0(t,x,k,a,\sigma) : x \cdot \exp(-k\cdot t) + (a-\sigma^2/4)\cdot\psi_k(k,t)$

$XCIR\_1(t,x,k,a,\sigma) : \max\left(\sqrt{x} + \sigma/2\cdot t, 0\right)^2$

$\tilde{X}(t,x,k,a,\sigma) : x + t\cdot\frac{\sigma}{\sqrt{2}}\cdot\sqrt{\left|a - \frac{\sigma^2}{4}\right|}$

generate_samples_Y(n) : random choice from $[\sqrt{3+\sqrt{6}}, -\sqrt{3+\sqrt{6}}, \sqrt{3-\sqrt{6}}, -\sqrt{3-\sqrt{6}}]$

with probabilities $\left[\frac{\sqrt{6}-2}{4\sqrt{6}}, \frac{\sqrt{6}-2}{4\sqrt{6}}, \frac{1}{2} - \frac{\sqrt{6}-2}{4\sqrt{6}}, \frac{1}{2} - \frac{\sqrt{6}-2}{4\sqrt{6}}\right]$

generate_samples_epsilon(n) : random choice from $[-1,1]$ with equal probabilities

generate_samples_zeta(n) : random choice from $[1,2,3]$ with equal probabilities

$K3(t,\sigma,a,k)$:

$\psi = \psi_k(-k,t)$

$$\alpha = \begin{cases} \left(\sqrt{\frac{\sigma^2}{4} - a + \frac{\sigma}{\sqrt{2}}\cdot\sqrt{a-\frac{\sigma^2}{4}}} + \frac{\sigma}{2}\cdot\sqrt{3+\sqrt{6}}\right)^2 & \text{if } 4a > \sigma^2 > \frac{4}{3}a \\ \frac{\sigma}{\sqrt{2}}\cdot\sqrt{a-\frac{\sigma^2}{4}} & \text{if } \sigma^2 \le \frac{4}{3}a \\ \frac{\sigma^2}{4} - a + \left(\sqrt{\frac{\sigma}{\sqrt{2}}\cdot\sqrt{\frac{\sigma^2}{4}-a}} + \frac{\sigma}{2}\cdot\sqrt{3+\sqrt{6}}\right)^2 & \text{otherwise} \end{cases}$$

return $\psi_k(-k,t)\cdot\alpha$

$\tilde{u}_3(t,x,a,k,\sigma)$:

$\psi = \psi_k(k,t)$

$\alpha = 2x^2 \cdot \exp(-2kt) + \psi_k(k,t) \cdot (a + \sigma^2/2) \cdot (3x \cdot \exp(-kt) + a \cdot \psi_k(k,t))$

return $\tilde{u}_1(t,x,a,k) \cdot \tilde{u}_2(t,x,a,k,\sigma) + \sigma^2 \cdot \psi_k(k,t) \cdot \alpha$

compute_pi_x_plus_minus(t,x,a,k,σ) :

$m1, m2, m3 = \tilde{u}_1(t,x,a,k), \tilde{u}_2(t,x,a,k,\sigma), \tilde{u}_3(t,x,a,k,\sigma)$

$s, p = \dfrac{m3 - m1 \cdot m2}{m2 - m1^2}, \dfrac{m1 \cdot m3 - m2^2}{m2 - m1^2}$

$\delta = s^2 - 4p$

$x\_plus, x\_minus = \dfrac{s + \sqrt{\delta}}{2}, \dfrac{s - \sqrt{\delta}}{2}$

$\pi = \dfrac{m1 - x\_minus}{x\_plus - x\_minus}$

return x_plus, x_minus, π

$\hat{X}\_xk0(t,x,k,K3\_t,Y,\sigma,\epsilon,\zeta)$:

temp, t, condition, mask_1, mask_2, mask_3 $= t, \psi_k(-k,t), (\sigma^2 \leq 4a), (\zeta == 1), (\zeta == 2), (\zeta == 3)$,

new_x = np.zeros_like(x)

if condition :

new_x[mask_1] $= \tilde{X}(\epsilon[mask\_1] \cdot t, XCIR\_0(t, XCIR\_1(\sqrt{t} \cdot Y[mask\_1], x[mask\_1], k, a, \sigma), k, a, \sigma), k, a, \sigma)$

new_x[mask_2] $= XCIR\_0(t, \tilde{X}(\ epsilon[mask\_2] \cdot t, XCIR\_1(\sqrt{t} \cdot Y[mask\_2], x[mask\_2], k, a, \sigma), k, a, \sigma), k, a, \sigma)$

new_x[mask_3] $= XCIR\_0(t, XCIR\_1(\sqrt{t} \cdot Y[mask\_3], \tilde{X}(\epsilon[mask\_3] \cdot t, x[mask\_3], k, a, \sigma), k, a, \sigma), k, a, \sigma)$

else :

new_x[mask_1] $= \tilde{X}(\epsilon[mask\_1] \cdot t, XCIR\_1(\sqrt{t} \cdot Y[mask\_1], XCIR\_0(t, x[mask\_1], k, a, \sigma), k, a, \sigma), k, a, \sigma)$

new_x[mask_2] $= XCIR\_1(\sqrt{t} \cdot Y[mask\_2], \tilde{X}(\epsilon[mask\_2] \cdot t, XCIR\_0(t, x[mask\_2], k, a, \sigma), k, a, \sigma), k, a, \sigma)$

new_x[mask_3] $= XCIR\_1(\sqrt{t} \cdot Y[mask\_3], XCIR\_0(t, \tilde{X}(\epsilon[mask\_3] \cdot t, x[mask\_3], k, a, \sigma), k, a, \sigma), k, a, \sigma)$

return $\exp(-k \cdot \text{temp}) \cdot$ new_x

generator_p_hat_x_3rdOrder$(t,x,K3_t,\sigma)$:

U, mask_smaller $=$ uniform random sample with shape x.shape, $(x \leq K3\_t)$

$x\_plus, x\_minus, \pi =$ compute_pi_x_plus_minus(t,x,a,k,σ)

return where(mask_smaller, where$(U \leq \pi, x_plus, x_minus), \hat{X}_xk0(t,x,k,K_3_t,$generate_samples_Y(len$(x))$, σ,

generate_samples_epsilon(len(x)), generate_samples_zeta(len(x)))))

6 Application to affine term structure models

6.1 An efficient scheme for the Heston model

In this section, we utilize the concepts previously established and adapt them to the Heston model. The Heston model, when the stock price is log-transformed, falls under the category of Affine Term Structure Models.

The theory established before is not applicable to the Heston model. This is primarily because the theory relies on discretization schemes with uniformly bounded moments, which assumes that the underlying SDE also possesses uniformly bounded moments. However, in the Heston model, the diffusion coefficient does not exhibit sublinear growth, leading to the explosion of moments within a finite time span. Consequently, the framework developed in this paper isn't suitable for providing a rigorous estimation of weak error within the Heston model. Nevertheless, it isn't futile to extend the

findings from Section 1 to the Heston model. The recursive construction of a second-order scheme offers a means to mitigate many biased terms of first order, thereby significantly enhancing convergence, as will be evident in the simulation phase.

We will then apply the results of Section 1 in a nonrigorous manner. To do so, we split the operator of the SDE (4.3) $L = LW + LZ$, where the two operators LW and LZ are associated to the following respective SDEs:

$$\text{For LW:} \quad \begin{cases} dX_t^1 = (a - kX_t^1)dt + \sigma\sqrt{X_t^1}dW_t, \\ dX_t^2 = X_t^1 dt, \\ dX_t^3 = (r - \frac{1}{2}(1-\rho^2)X_t^1)X_t^3 dt + \rho\sqrt{X_t^1}X_t^3 dW_t, \\ dX_t^4 = X_t^3 dt. \end{cases}$$

$$\text{For LZ:} \quad \begin{cases} dX_t^1 = 0, \\ dX_t^2 = 0, \\ dX_t^3 = \sqrt{(1-\rho^2)X_t^1}X_t^3 \circ dZ_t, \\ dX_t^4 = 0. \end{cases}$$

Here, $\circ$ denotes the Stratonovitch integral. The second SDE is easy to integrate exactly and we denote by $\hat{p}_Z(t,x)$ the exact scheme. For $x = (x_1, x_2, x_3, x_4) \in \mathbb{R}^4$, $p_Z(x,t)$ is simply the law of $(x_1, x_2, x_3 \exp(tx_1(1-\rho^2)N), x_4)$, where $N \sim N(0,1)$.

Concerning the first SDE, we use the second or the third order scheme described in this paper for the CIR. To discretize X_t^2, we then use the construction of Theorem 1.17 with the exact scheme for $x_2\partial_1$, which amounts to using the trapezoidal rule. Then, we observe that X^3 can be integrated exactly in functions of the increments of X^1 and X^2:

$$X_t^3 = X_0^3 \exp\left((r - \frac{\rho}{\sigma}a)t + \left[\frac{\rho}{\sigma}k - \frac{1}{2}\right](X_t^2 - X_0^2) + \frac{\rho}{\sigma}(X_t^1 - X_0^1)\right),$$

and we use this formula with the increments of the discretization. Finally, we discretize X^4 like X^2 using the trapezoidal scheme. To sum up, let $\hat{X}_{CIR}^1(t)$ denote a random variable sampled using either the second or the third order scheme for the CIR given in Theorems 2.8 and 3.7, with a time step $t > 0$ and starting from $x_1 \geq 0$. Here, we consider for LW the scheme $\hat{p}_W(x,t)$ defined as the law of

$$\begin{pmatrix} \hat{X}_{x_1}^{CIR}(t) \\ x_2 + \frac{x_1 + \hat{X}_{x_1}^{CIR}(t)}{2}t \\ x_3\xi_{x_1}(t) \\ x_4 + \frac{x_3(1+\xi_{x_1}(t)}{2}t \end{pmatrix}, \tag{15}$$

where

$$\xi_{x_1}(t) = \exp\left((r - \frac{\rho}{\sigma}a)t + \left(\frac{\rho}{\sigma}k - \frac{1}{2}\right)\frac{x_1 + \hat{X}_{x_1}^{CIR}(t)}{2}t + \frac{\rho}{\sigma}(\hat{X}_{x_1}^{CIR}(t) - x_1)\right).$$

Then, to approximate the diffusion (4.3), we finally consider the scheme

$$\hat{p}_x(t) = \frac{1}{2}(\hat{p}_W(t) \circ p_Z(x,t) + \hat{p}_Z(t) \circ p_W(x,t)). \tag{16}$$

7 Simulation results

7.1 Simulations and comparisons Euler's scheme and Ninomiya and Victoir's scheme

In this section, we study the following schemes:

- Euler-Maruyama with Monte Carlo
- Euler-Maruyama with Romberg extrapolation and with Monte Carlo

- Ninomiya and Victoir with Monte Carlo
- Ninomiya and Victoir with Romberg extrapolation and Monte Carlo
- Euler-Maruyama with Quasi-Monte Carlo
- Euler-Maruyama with Romberg extrapolation and with Quasi-Monte Carlo
- Ninomiya and Victoir with Quasi-Monte Carlo
- Ninomiya and Victoir with Romberg extrapolation and Quasi-Monte Carlo

7.1.1 Results a function of the strike

First, we decided to modify the strike of the Asian Call to see the results of the different schemes.

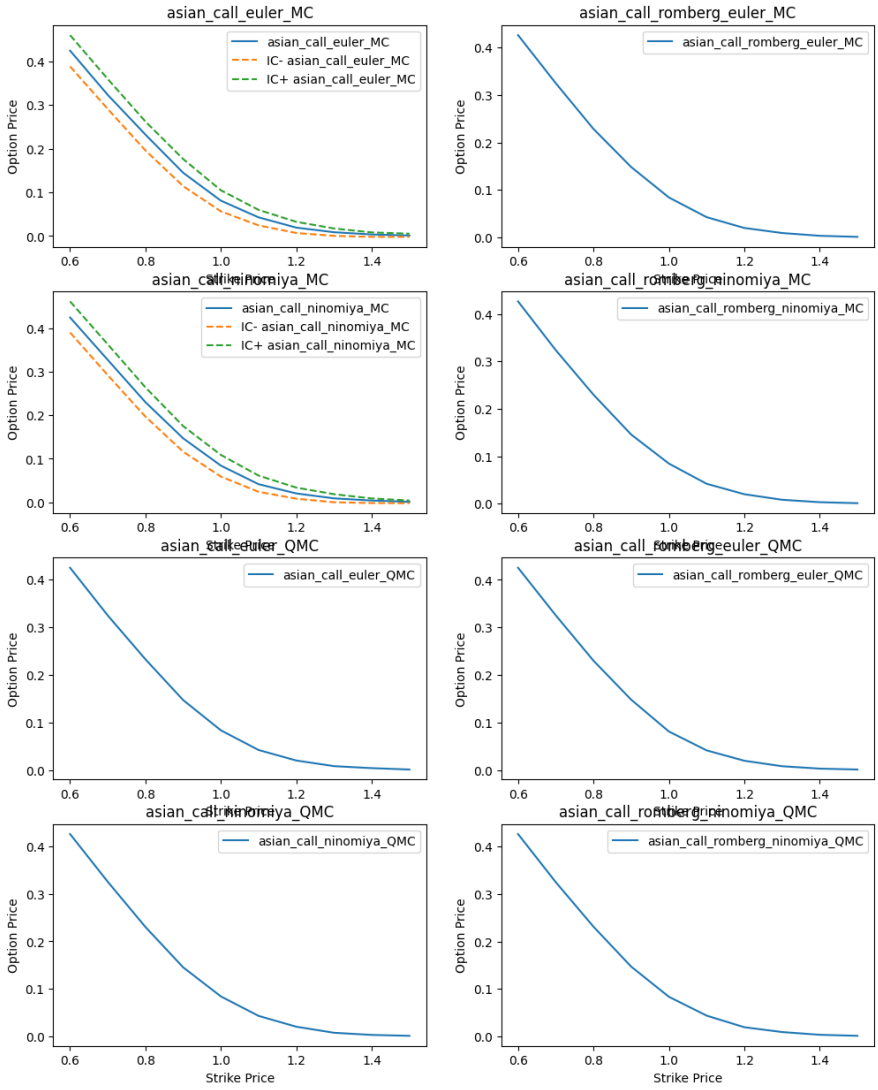

Figure 1: Evolution of the option price with respect to the strike for our different schemes

We notice than all our schemes give the same results for our Asian Call option. This confirms that they are all adapted for this kind of stochastic process. The convexity of the Call is also present (with a price decreasing to 0 when the strike increases.

7.1.2 Execution time

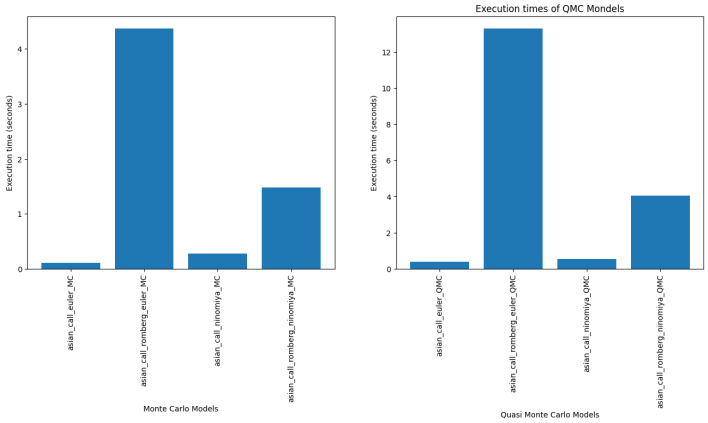

Figure 2: Execution times for a number of points of 10^2 and a number of paths of 10^4 for our different schemes

We can make several observations:

- Firstly, QMC methods do indeed take longer to execute for the same number of points (unsurprisingly, since they are designed to be executed with fewer points than MC methods).
- The two diagrams are similar in terms of proportions. Indeed, the classic Euler diagram is the faster, while the Euler diagram with Romberg extrapolation is the longer.
- We also note that Ninomiya and Victoir's scheme performs very well (it has a low execution time even with Romberg extrapolation).

7.1.3 Comparison of the convergence error between the schemes

To compare our different schemes, we can also observe their convergence error. To do this, the article by Ninomiya and Victoir proposes setting this error at 2σ when the standard deviation is one-way (i.e. when we use a Monte Carlo simulation). When we use a QMC method, we don't have a confidence interval, and the article suggests looking at the absolute value of the difference between the price of the scheme and a price of $6.0473907415 * 10^{-2}$. This is highly open to criticism, since this value was also obtained by QMC simulation.

We then vary the number of discretization points. Here are the results we obtain:

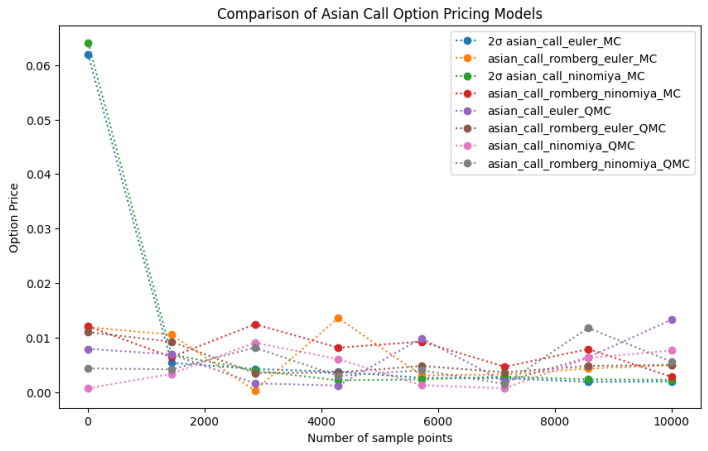

Figure 3: Comparison of the convergence error of the different schemes

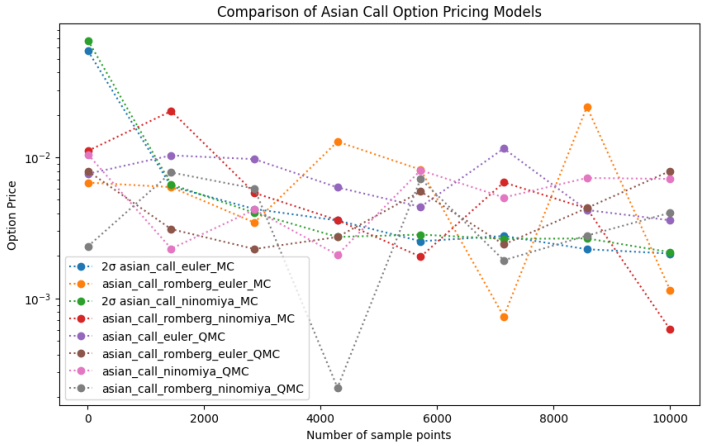

Figure 4: Comparison of the convergence error with log scale

We note that the convergence error clearly decreases with the number of discretization points. When we look back at the performance of these schemes, we notice that the Ninomiya and Victoir with Romberg extrapolation MC, but also Ninomiya and Victoir with Romberg extrapolation QMC schemes do indeed appear lower on the graph than the others. Although this difference is less obvious than in the paper of Ninomiya and Victoir, it is still present in our simulations.

7.1.4 Comparison of confidence intervals between Euler-Maruyama and Ninomiya schemes

It is important to remember that, when we run a Monte Carlo simulation, we have the confidence interval, without any further calculations. One of the difficulties is to reduce this confidence interval, and thus reduce the variance.

In both the Euler-Maruyama and Ninomiya schemes, we draw Gaussian variables. Now, if $Z\mathcal{N}(0,1)$, then, $Z \sim -Z$. So, one method of variance reduction that presents itself to us is to use the method of antithetic variables.

Here are the results we get when we implement it:

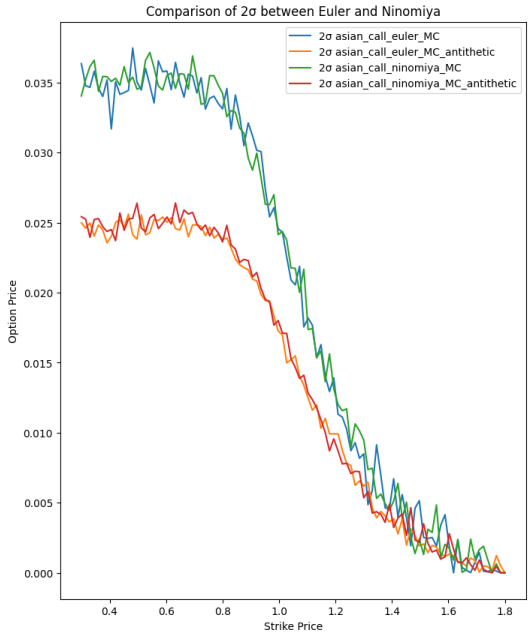

Figure 5: Comparison of 2σ between Euler and Ninomiya schemes (with and without variance reduction)

We can make several observations:

- Firstly, the antithetic variables method works on both schemes. Indeed, this method reduces the confidence interval, especially for small Strike values.
- The general shape of the curve is the same for both schemes, with a standard deviation that seems to stagnate at a fixed value for small Strike values.
- Finally, we also note that neither scheme seems better than the other in terms of confidence intervals.

7.2 Simulations for the CIR process

In this section, we depict the convergence of both second and third-order schemes for the CIR model, focusing on cases where existing discretization schemes struggle due to $\sigma^2 < 4a$, as noted earlier. Schemes 1 and 2, recommended by Alfonsi, represent the second and third-order schemes respectively, with their simulations depicted by solid lines in Figure 1. Additionally, we explore three variations of the second-order scheme to highlight the significance of the threshold $K_2(t)$, which dictates when to switch between schemes. We examine whether choosing thresholds smaller than $K_2(t)$, ensuring non-negativity by using positive parts, results in second-order schemes or potentially inferior ones.

1. Second order scheme with switching threshold $\frac{3}{2}K_2(t)$.
2. Second order scheme with switching threshold $\frac{K_2(t)}{2}$, forcing nonnegativity with positive parts.
3. Second order scheme with $N \sim \mathcal{N}(0,1)$ instead of Y, forcing nonnegativity with positive parts.

We set $T = 1$ and plot $E(\exp(-\tilde{X}_n t_n/n))$ against $1/n$ for two parameter sets: $\sigma^2 < 4a$ (left) and $\sigma^2 \geq 4a$ (right). When $\sigma^2 < 4a$, most schemes stay above the switching threshold, explaining why we observe no differences between schemes 1, 3, and 4. Scheme 5 shows qualitatively quadratic convergence and is slightly better than scheme 1. Third-order scheme 2 converges much better, reaching five-digit precision by $n = 5$.

When $\sigma^2 \geq 4a$, the discussion on the threshold becomes more intriguing as schemes often hover around this value. Schemes 1 and 2 converge as expected, with scheme 2 outpacing scheme 1. Scheme 3 converges with quadratic speed, but slightly downgrades compared to scheme 1 with increasing threshold. Despite theoretically allowing any $\tilde{K}(t)$ greater than $K_2(t)$ to yield a second-order scheme, it's better to choose the smallest, as in scheme 1. Scheme 4's erratic behavior highlights the real impact of $K_2(t)$ on convergence. Additionally, scheme 5's convergence deteriorates with smaller time steps compared to schemes 1 and 3.

Table 1: Results for scheme 3. Parameters as in Figure 4. Precision up to two standard deviations: 5×10^{-4}.

n	5	7	10	14	20	30	50
$E(\exp(-\tilde{X}_n t_n/n))$	4.6189	4.4427	4.3108	4.2235	4.1570	4.1062	4.0646

7.2.1 Simulations for the Heston model

In this section, we evaluate scheme (4.5) for pricing claims under the Heston model. Scheme 1 (resp. 2) employs the second (resp. third) order scheme for the nested CIR in (4.4). We explore whether using the third-order scheme for the CIR offers advantages over the second-order one. Additionally, we introduce scheme 3, coinciding with that suggested by Lord et al. [18] for the first and third coordinates.

$$X_t^x = \begin{pmatrix} x_1 + (a - kx_1^+)t + \sigma\sqrt{x_1^+}W_t \\ x_2 + x_1 t \\ x_3 \exp\left((r - \frac{x_1^+}{2})t + \sqrt{x_1^+}(\rho W_t + \sqrt{1-\rho^2}Z_t)\right) \\ x_4 + x_3 t \end{pmatrix}$$

For all simulations, $T = 1$. European put prices for different strikes with relatively high σ are calculated in Figure 2 and Figure 3. While it's hard to discern whether convergence is quadratic for schemes 1 and 2 from the curves, comparing values with exact ones reveals promising results, especially for scheme 2 when $\sigma^2 \geq 4a$. Scheme 3 exhibits rather linear convergence in these scenarios. Figure 4 illustrates the prices of an Asian put and an exotic option, showcasing the difference in convergence behavior between scheme 2 and scheme 3. Table 2 shows values obtained with scheme 3 for the Asian option, emphasizing its quasi-linear convergence.

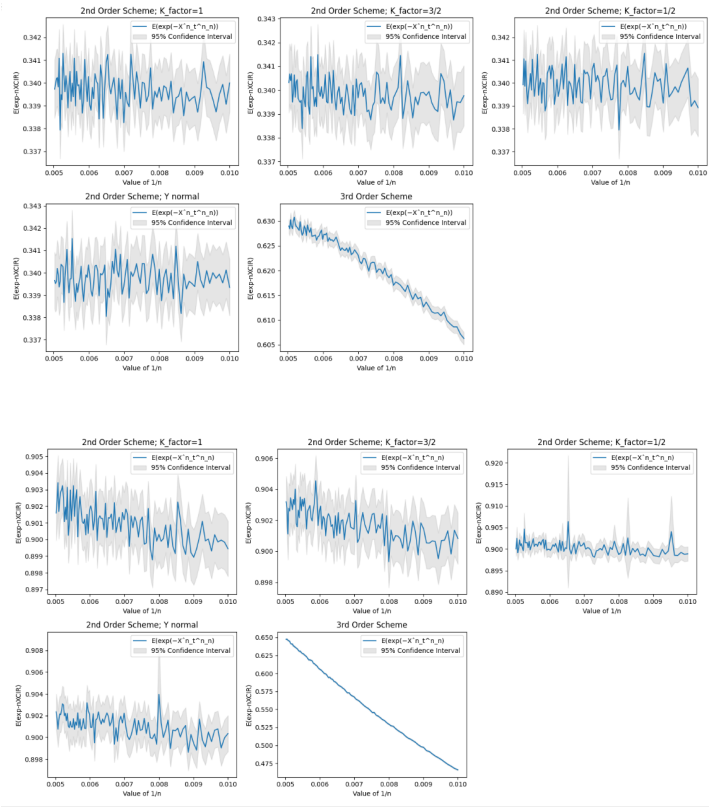

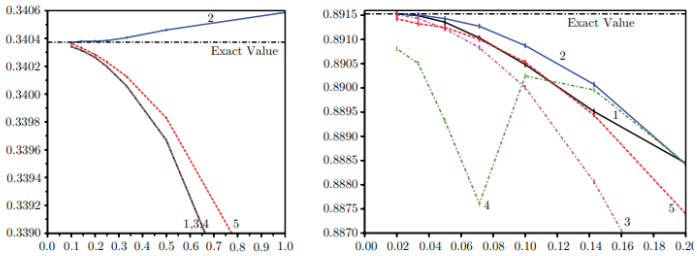

FIGURE 1. $\mathbb{E}(\exp(-\hat{X}^n_{t^n_n}))$ as a function of $1/n$ with $x_0 = 3/2$, $k = 1/2$, $a = 1/2$ and $\sigma = 0.8$ (left) and $x_0 = 0.3$, $k = 0.1$, $a = 0.04$ and $\sigma = 2$ (right). The width of each point gives the precision up to two standard deviations.

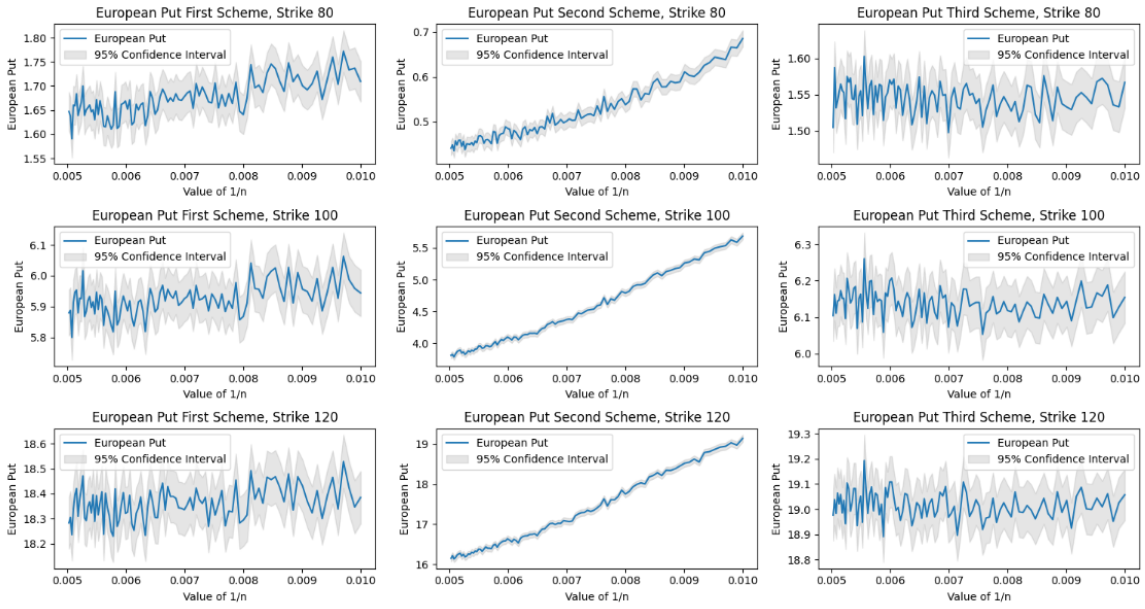

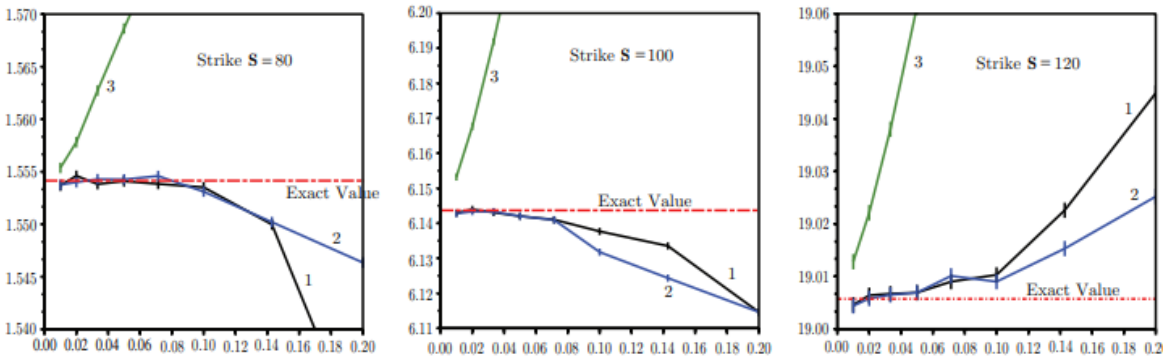

FIGURE 2. $\mathbb{E}[e^{-r}(\mathbf{S} - (\hat{X}^n_{t^n_n})_3)^+]$ as a function of $1/n$ with $X^1_0 = 0.04$, $k = 0.5$, $a = 0.02$, $\sigma = 0.4$, $r = 0.02$, $X^3_0 = 100$ and $\rho = -0.5$. The point width gives a 95% confidence interval.

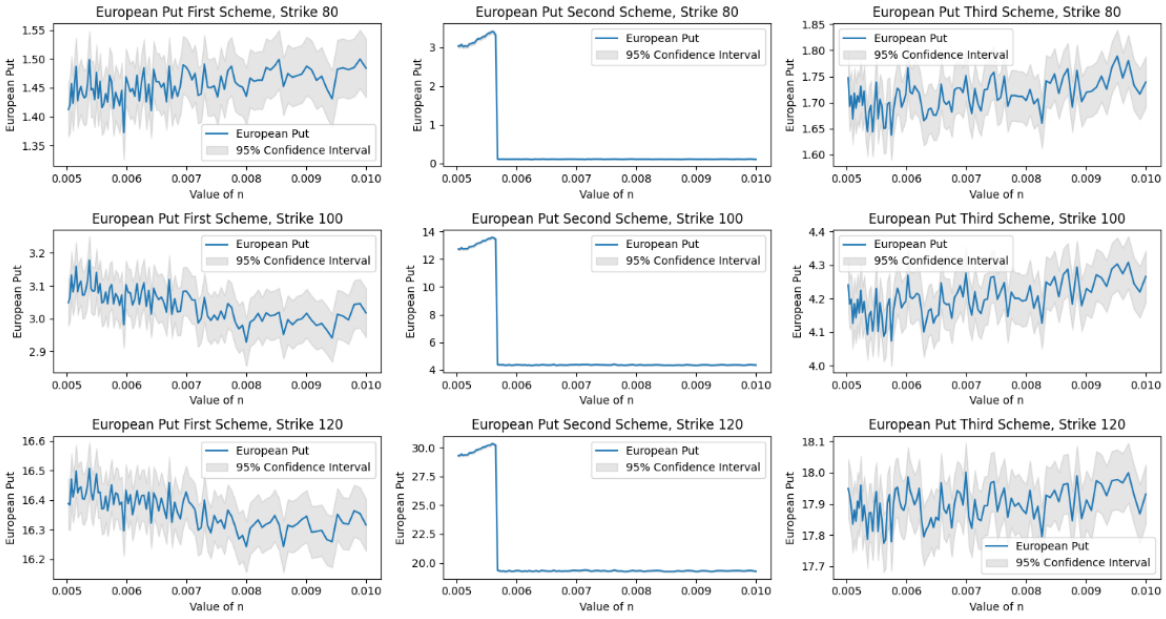

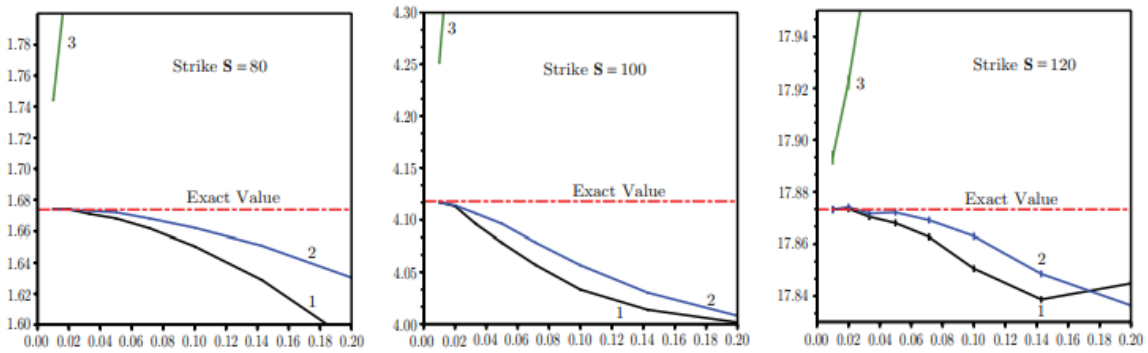

FIGURE 3. $\mathbb{E}[e^{-r}(\mathbf{S} - (\hat{X}^n_{t^n_3})_3)^+]$ as a function of $1/n$ with $X^1_0 = 0.04$, $k = 0.5$, $a = 0.02$, $\sigma = 1$, $r = 0.02$, $X^3_0 = 100$ and $\rho = -0.8$. The point width gives a 95% confidence interval.

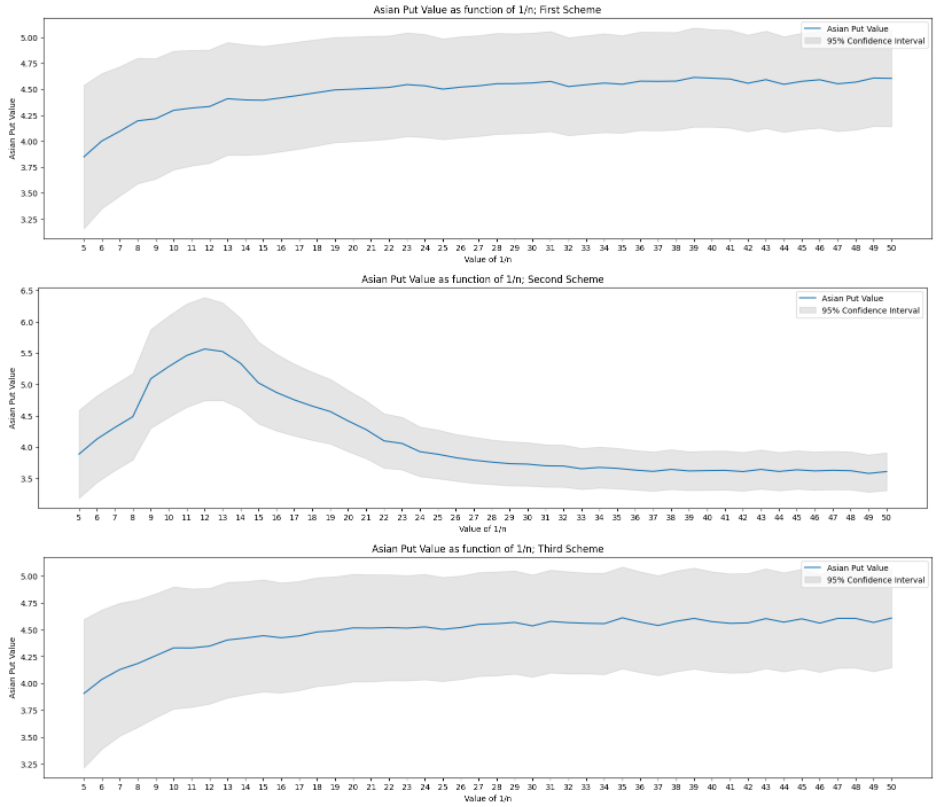

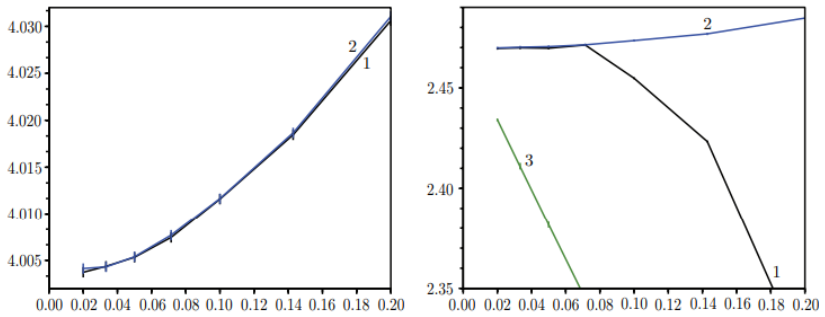

FIGURE 4. Plots of $\mathbb{E}[e^{-r}(100 - (\hat{X}^n_{t^n_n})_4)^+]$ (left) and $\mathbb{E}[e^{-r}\mathbf{1}_{(\hat{X}^n_{t^n_n})_2 > a/k}((\hat{X}^n_{t^n_n})_4 - (\hat{X}^n_{t^n_n})_3)^+]$ (right) as a function of the time step $1/n$ with $X^1_0 = 0.04$, $k = 0.5$, $a = 0.02$, $\sigma = 0.2$, $r = 0.02$, $X^3_0 = 100$ and $\rho = -0.3$. The point width gives the two standard deviation precision.

References

[Alf10] Aurélien Alfonsi. High order discretization schemes for the cir process: application to affine term structure and heston models. *Mathematics of Computation*, 79(269):209–237, 2010.

[NV08] Seishi Ninomiya and Nicolas Victoir. Weak approximation of stochastic differential equations and application to derivative pricing. *Applied Mathematics & Finance*, 15(2):107–121, 2008.